# Pyridine Gold Complexes. An Emerging Class of Luminescent Materials

**Eduardo J Fernández[1], Antonio Laguna[2], José M López-de-Luzuriaga[1], Miguel Monge[1] , Manuel Montiel[1], M Elena Olmos[1], Javier Pérez[1], and María Rodríguez-Castillo[1]**

[1] Departamento de Química, Universidad de La Rioja, Grupo de Síntesis Química de La Rioja, U.A.-CSIC. Madre de Dios 51, E-26006 Logroño, Spain
[2] Departamento de Química Inorgánica, Instituto de Ciencia de Materiales de Aragón, Universidad de Zaragoza-CSIC, E-50009 Zaragoza, Spain
E-mail: alaguna@unizar.es

Dedicated to Prof. Juan Fornies on the occasion of his 60th birthday.

## Abstract

**Pyridine-type ligands are considered one of the most versatile ligands in photochemistry since they can act as emitters themselves or as donor or acceptors of electronic density depending on the electronic character of the substituents of the rings and the metal centers bonded to them. Gold is a well known metal with an impressive tendency to form metal aggregates through metal-metal interactions and, therefore, gold complexes bearing these ligands are tailored derivatives with potential as emitting materials. The new possibilities of experimental and theoretical studies that appear with the easy synthesis of a new class of luminescent materials formed by the combination of pyridine ligands and gold are shown here.**

## Introduction

One of the most used ligands in the coordination chemistry of the transition metals are the pyridine-type ligands, not only for their coordination abilities but also because they promote in many cases very interesting photophysical properties.[1] However, the number of gold pyridine[2a] or heterocyclic amine[2b,2c] complexes is limited and, as far as we know, there is no report on the luminescent properties of such complexes. An enormous unexplored potential exists in this type of molecules and the synthesis and stability of simple organometallic gold(I) mononuclear systems may not offer any problem.

Gold is an element that, in spite of having a closed shell configuration, displays unexpected characteristics as its obstinate tendency to form aggregates through metal-metal interactions.[3] This phenomenon was termed '*aurophilicity*' by Schmidbaur in the eighties[4] and nowadays it is considered responsible, among others, for the optical properties that many gold complexes display.

In this sense, the great number of studies carried out has allowed us to know the conditions that a gold complex requires to show luminescence. These can be summarized in the short metal-metal interactions, the geometry around the metal center or the nature of the ligands that can act as donors or acceptors of electronic density or themselves in internal transitions, usually among $\pi$ orbitals.[5]

We have also worked in another class of luminescent gold-heterometal materials that behave as luminescent systems as a result of the metal-metal interactions.[6] To build these it is possible to make use of an acid-base strategy in which bis(perhalophenyl)gold(I) anions react with Lewis acids as silver or thallium. The results of the reactions depend on the heterometal as well as the perhalophenyl group bonded to gold, giving rise to extended polymetallic chains or discrete molecules with a great variety of metal-metal interactions and optical properties, which depend on them.

In summary, in spite of the apparent simplicity of the conditions that a gold complex requires to show luminescence, there are many factors that can occur in a gold complex at the same time and it is difficult to systematize.

At this point we wondered whether the use of the starting material $[Au(C_6Cl_5)(tht)]$ (tht = tetrahydrothiophene labile ligand) against 4-substituted pyridine ligands would be a method of choice for the synthesis of discrete gold(I) luminescent materials. We have chosen these type of molecules since in spite of their simplicity a deep study on their photophysical behavior from experimental and theoretical viewpoints would be carried out. Indeed, as it is known, the use of perhalophenyl ligands bonded to gold confers a great stability to the new compounds due to stronger carbon-metal bond formation.

Hence, in this paper we report the synthesis of new $[Au(C_6Cl_5)(4\text{-}X\text{-}Py)]$ (X=MeO- (**1**), Me- (**2**), $^t$Bu- (**3**), H- (**4**), COOMe- (**5**) and CN- (**6**)) complexes and the study of their luminescent properties. Thus, we have analysed how the changes on the

**Scheme 1**

*Synthesis of complexes 1-6*

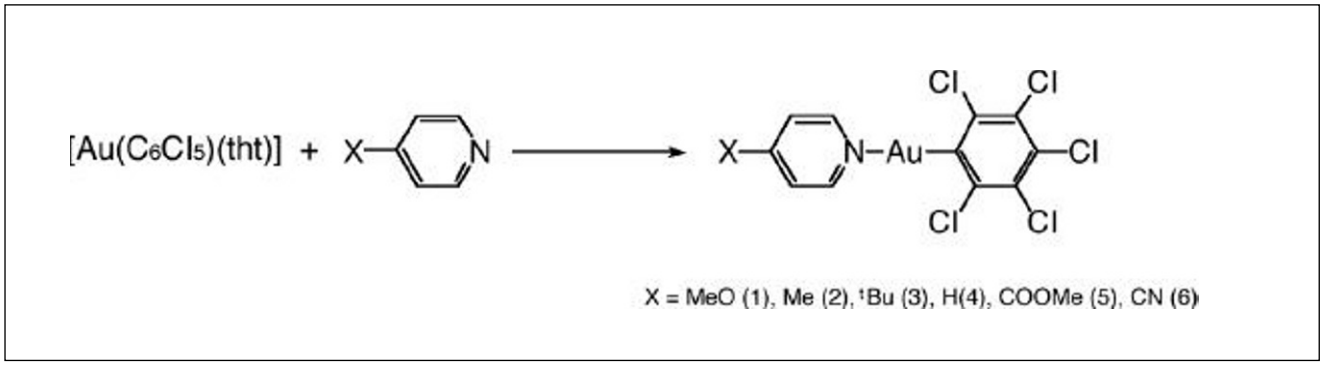


donor properties of the subsituent in the 4-position of the pyridine ligands affect the photophysical properties of the gold complexes. Moreover, these photophysical properties have been studied from a theoretical viewpoint by the use of DFT calculations that permit us to check the influence not only of the changes on the substituents of the pyridine ligands but also the influence of the presence of gold-gold interactions or even the structural disposition between two mononuclear units in parallel or antiparallel alignment.

## Organometallic gold(I) 4-substituted pyridine compounds

By conventional reactions of the perhalophenyl gold(I) precursor with 4-substituted pyridines in a 1:1 molar ratio, the corresponding gold-pyridine complexes are prepared in high yields. All of these complexes show a great stability to air and moisture.

Complexes **1-5** are white solids and complex **6** is a yellow solid and all of them are soluble in most common organic solvents as dichloromethane, acetone, toluene, acetonitrile, etc. and insoluble in *n*-hexane. The analytical and spectroscopic data are in accordance with the proposed stoichiometries. In this sense, the $^{1}H$ NMR spectra of all complexes confirm the coordination of the pyridine ligands to gold(I) through the shifts of the signals of the aromatic protons of the pyridine ligands to down field.

## Nature of the ligands

To understand the reactivity between [Au($C_6Cl_5$)(tht)] and the different pyridines and their electronic behaviour the electron density mapped with electrostatic potential (ESP) of all them were obtained. We have used [Au($C_6Cl_5$)($SH_2$)] as a model system that represents the gold precursor in which we have substituted the tetrahydrothiophene ligand (tht) by $SH_2$ in order to save computational costs. Regarding free 4-substituted pyridines we have analyzed the ones with methoxy, methyl, hydrogen or cyano as substituents.

The obtained density maps reveal that in the perchlorophenyl gold precursor complex, the aryl group bear

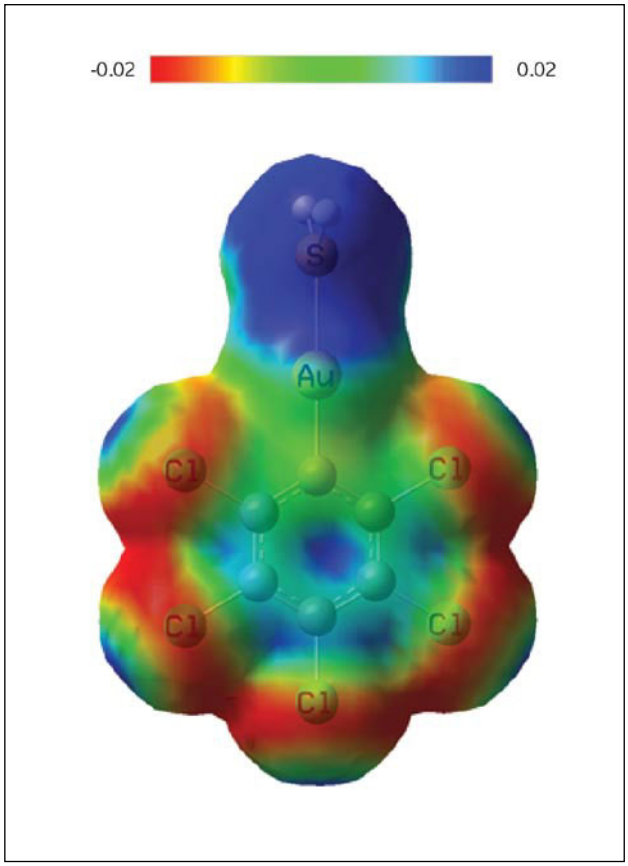


**Figure 1**

*Electron density from the total SCF density (isoval = 0.02) mapped with the electrostatic potential (ESP) for model system [Au($C_6Cl_5$)($SH_2$)]*

**Table 1**

*Spectroscopic and photophysical properties of complexes **1-6***

| Complex | max.$\lambda_{abs}$[nm] ($\varepsilon$[$mol^{-1}dm^3cm^{-1}$])[a] | $\lambda_{em}(\lambda_{exc})$[nm]/$\tau$(μs)[b] |
|---|---|---|
| **1** | 229 (2240) | 463(372)/11.1 |
| **2** | 255 (2593) | 490(370)/9.8 |
| **3** | 256 ( 4792) | 506(365)/9.8 |
| **4** | 251 (2451) | 514(369)/10.2 |
| **5** | 272 (2616) | 516(366)/11.3 |
| **6** | 272 (2263) | 547(370)/10.0 |

[a]: In dichloromethane at 298 K; b: solid at 298 K

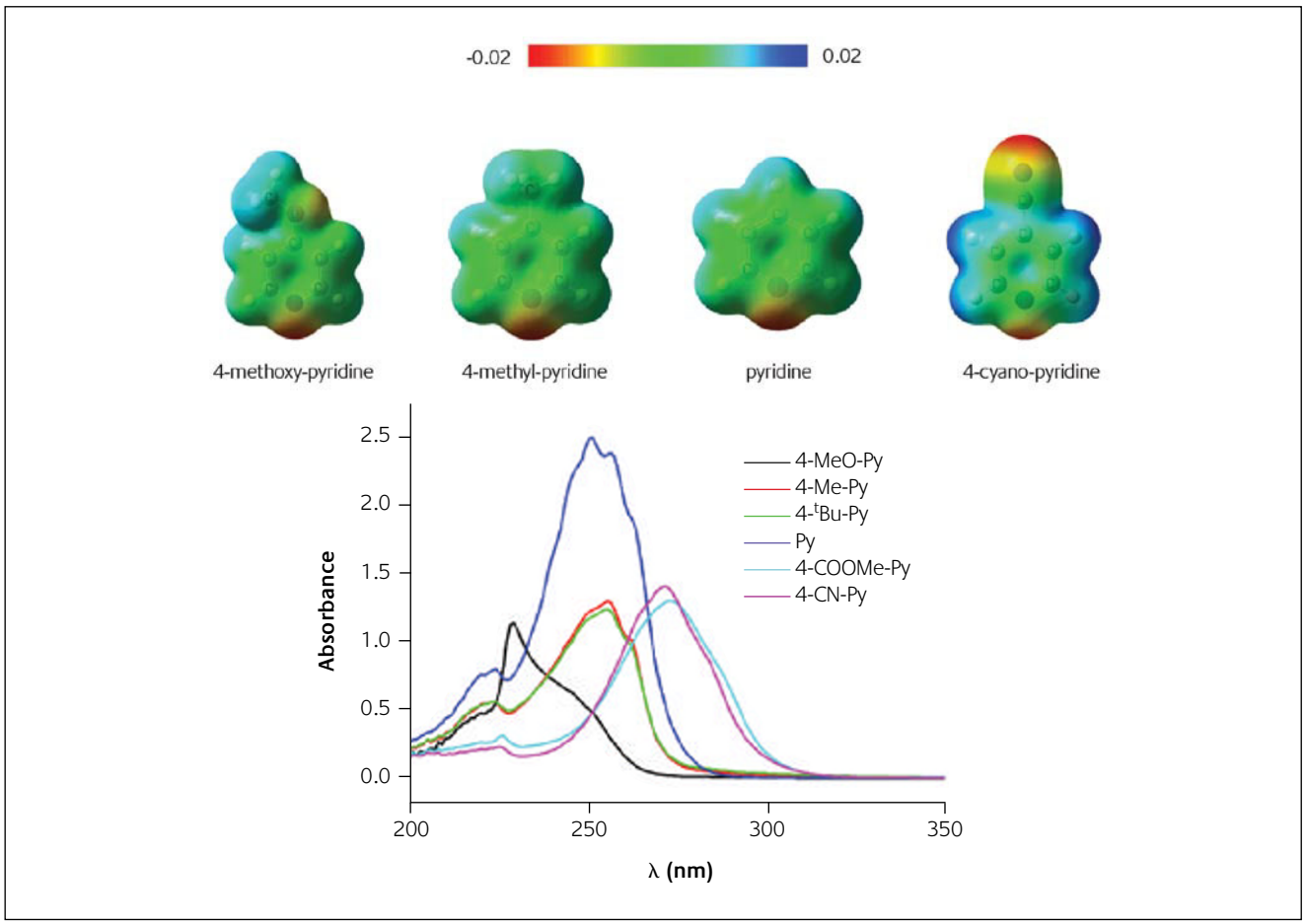


**Figure 2**

*Electron density from the total SCF density (isoval = 0.02) mapped with the electrostatic potential (ESP) (top) and UV-Vis spectra in 5x10$^{-4}$ M $CH_2Cl_2$ solutions (bottom) for free 4-substituted pyridine ligands*

the negative charge of the complex, the $SH_2$ that models the tht ligand the positive one, and the gold center acts almost as a neutral connection between both, giving rise to highly polar molecules in which charge transfer transitions are predictable.

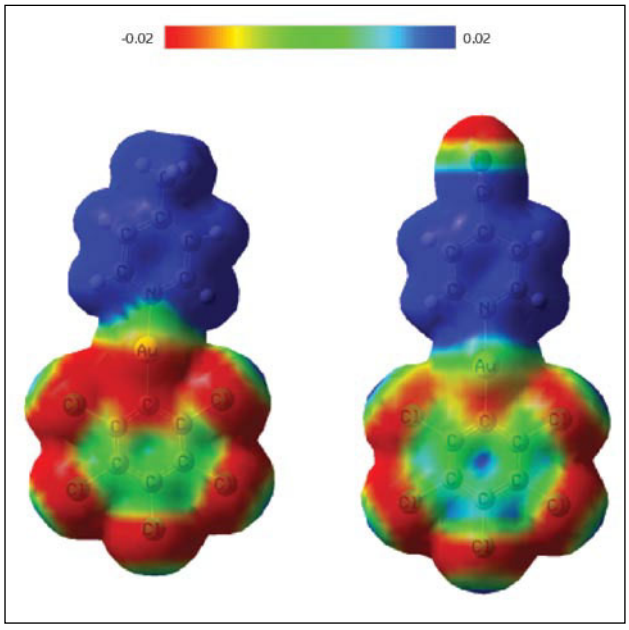


**Figure 3**

*Electron density from the total SCF density (isoval = 0.02) mapped with the electrostatic potential (ESP) for model systems [Au($C_6Cl_5$)(4-Me-Py)] and [Au($C_6Cl_5$)(4-CN-Py)]*

As we have mentioned before, among the ligands that can act as acceptors of this electronic density, 4-substituted pyridines have been chosen, because they show empty π orbitals and the substituent in position 4 can modulate the accepting abilities of these ligands. In fact, the broad bands that appear in the ultraviolet-visible spectra of the pyridines (Table 1) in dichloromethane appears at high energy (225-275 nm) with tails extended to ca. 300 nm in the case of the 4-cyano- and 4-isonicotinate-pyridine. These absorptions are assigned to π–π* transitions located in the rings and, as expected, the energy of the maxima of these roughly shift to red as the accepting ability of the substituent increases (for example 229 nm for the MeO-Py and 272 nm for the CN-Py), in agreement with the changes observed in the calculated electron density maps for selected 4-substituted pyridines.

In the same way, by the calculation of the electron density maps of two examples of [Au($C_6Cl_5$)(4-X-pyridine)] (X = Me (2) and CN (6)) complexes we can observe that the reaction between pyridine ligands and the perhalophenyl gold(I) precursor produces highly polar molecules in which, depending on the substituent of the pyridines the polarization is higher. The principal aim in these reactions is that these molecules are promising candidates for charge transfer transitions.

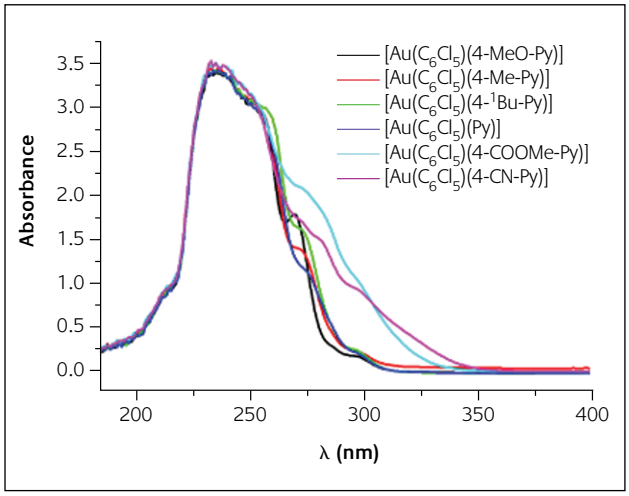


**Figure 4**

*UV-Vis spectra of complexes **1-6** in 5x10$^{-4}$ M $CH_2Cl_2$ solutions*

Indeed, the experimental spectroscopic data of the complexes confirm those assumptions. The ultraviolet-visible spectra of the perchlorophenyl complexes show a common band of high intensity at 240 nm, which is common for all the complexes and which is characteristic of allowed $\pi$–$\pi^*$ transitions located in the perchlorophenyl ring,[7] although it can be observed a similar tendency in the band edge than in the free pyridines. Thus, the absorptions shift to red when the substituents of the pyridines in position 4 increase its electron-accepting abilities.

In the same way, the emission spectra of the complexes, in solid state at room temperature, display in all cases very strong bands whose positions depend on the pyridine ligand. The energies of the emissions are in accordance with the commented tendency and, therefore, the cyano-pyridine derivative appears at the lowest energy and the methoxy-pyridine complex at the highest one, the rest of them following a consequent sequence. This result is in accordance with charge transfer transitions between orbitals of the electron rich perchlorophenyl group and the pyridine ligands and, therefore, when the substituents of the pyridine increase its electron accepting abilities the transition from the perchlorophenyl group is more favoured and, consequently the emissions shift to red. These cover a range between 463 nm to 547 nm or from blue to yellow greenish.

## Structural analysis

Single crystals of complexes **2**, **3**, **4** or **6** suitable for X-ray diffraction studies were obtained by slow diffusion of n-hexane into a solution of complexes in dichloromethane. Tables 2 and 3 contain the data collection and refinement details and selected bond distances and angles. In the case of complex **2**, crystals of two different polymorphs were obtained depending on the solvents employed in the crystallization process: $CH_2Cl_2$/hexane (**2a**) or toluene/hexane

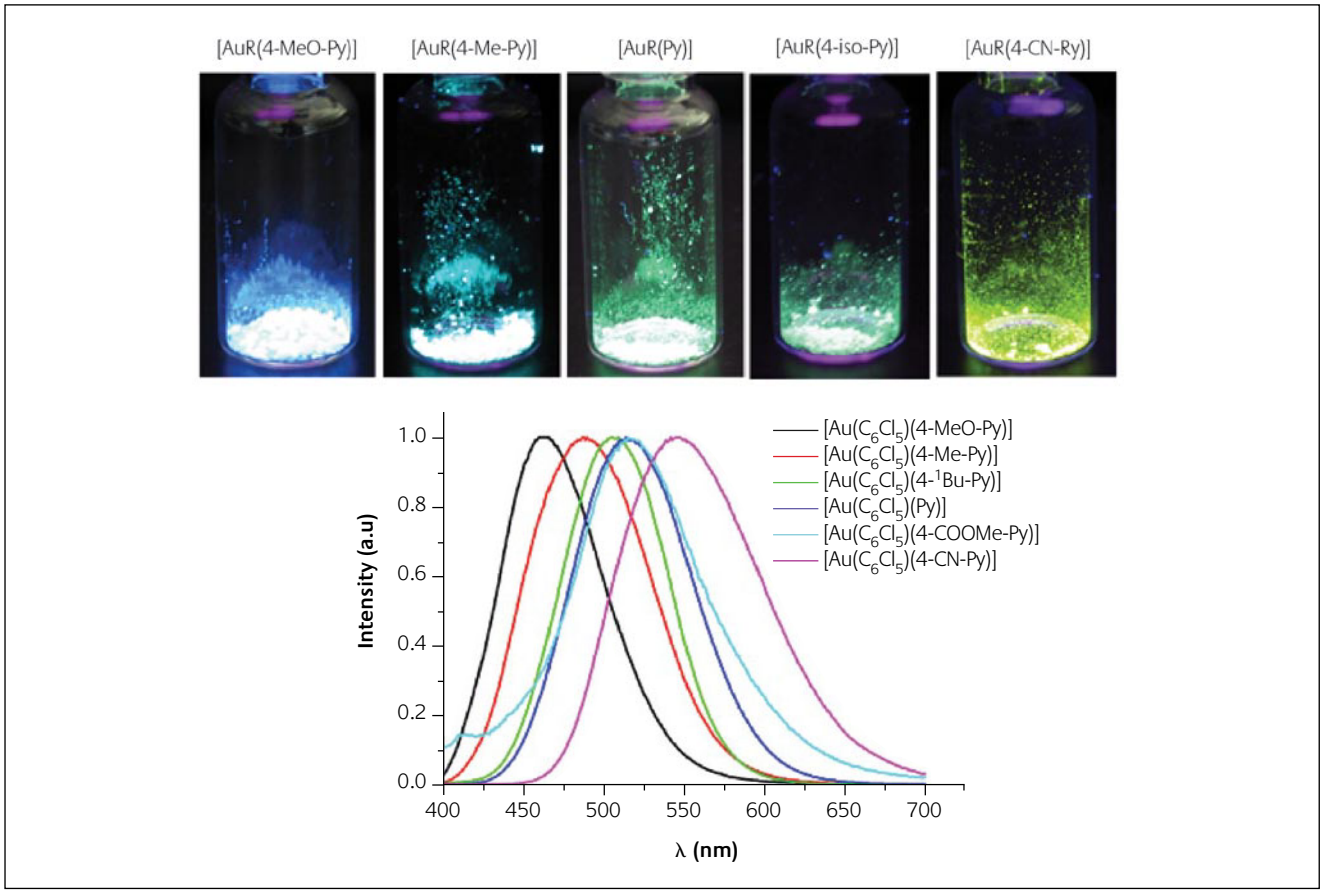


**Figure 5**

*Emission spectra of complexes **1-6** in solid state at room temperature*

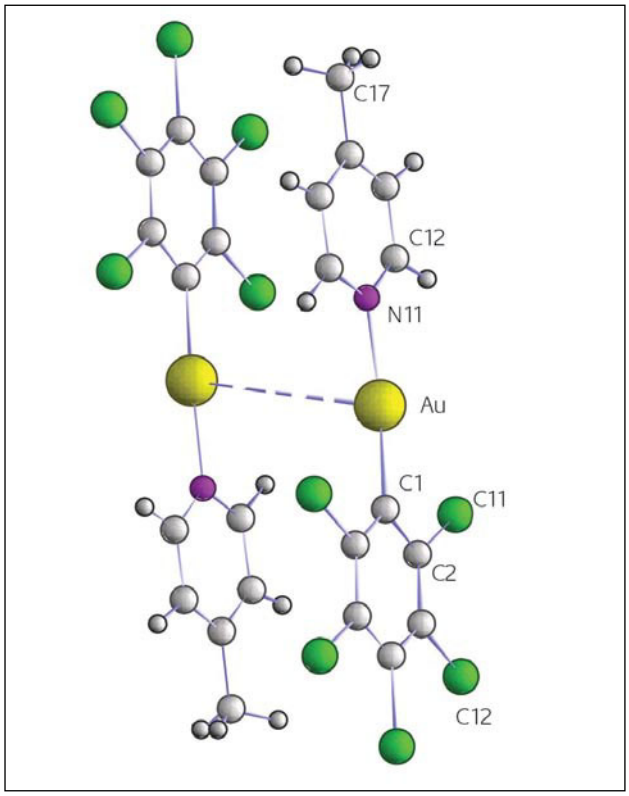


**Figure 6**
*Crystal structure of complex **2a***

(**2b**). All the crystal structures show [Au($C_6Cl_5$)(4-X-pyridine)] molecules containing a linearly coordinated gold(I) atom with a maximum deviation from linearity of 4.2° in **2a** and typical Au-C and Au-N bond distances that range from 1.989(8) to 2.031(8) Å and from 2.062(7) to 2.085(7) Å, respectively.

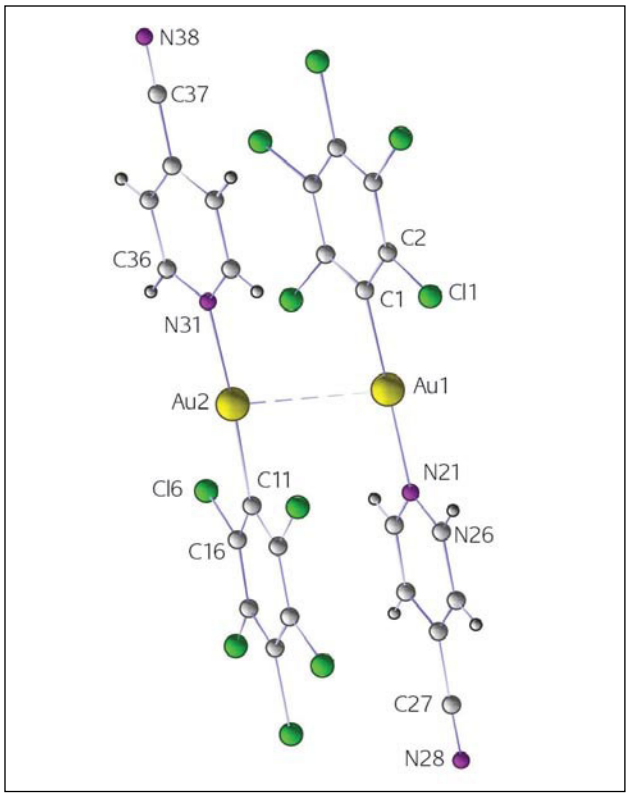


**Figure 8**
*Crystal structure of complex **6***

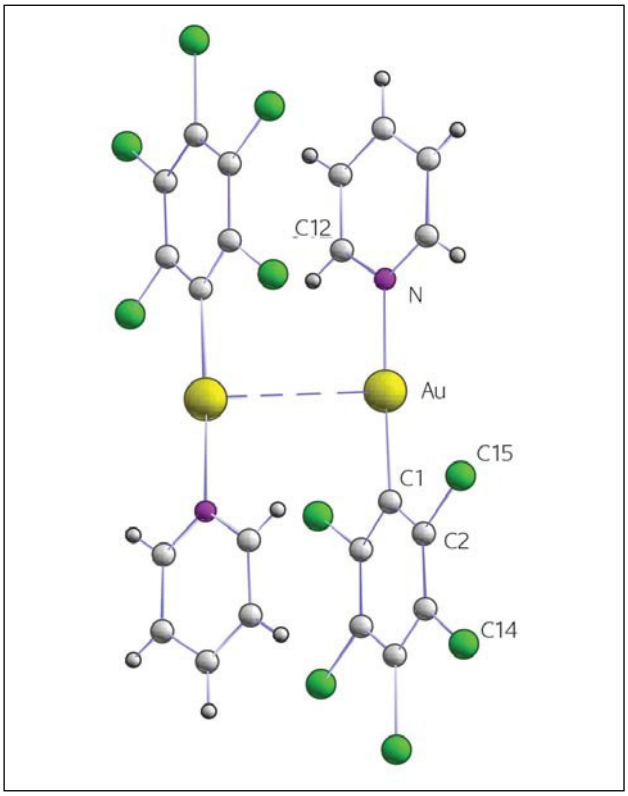


**Figure 7**
*Crystal structure of complex **4***

The main difference between the solid state structures of these compounds is found when intermolecular interactions, mainly aurophillic contacts, and the packing of the molecules are analysed. Thus, three different dispositions of molecules are observed in the net: extended chains of molecules in an antiparallel disposition that are associated in couples via a very weak unsupported Au...Au contact, extended chains of isolated molecules in a parallel disposition, and chains of couples of molecules (joined via an unsupported aurophillic interaction) in a nearly antiparallel fashion and without contacts between couples.

The most common structure is the first one, which is found in one of the polymorphs of **2** (**2a**) and in complexes **4** and **6**. In these three cases the pentachlorophenyl and pyridine rings of each molecule are nearly coplanar forming an angle of 3.48, 13.23 or 14.13° for **2a**, **4** or **6**, respectively, and a weak metallophilic unsupported interaction of 3.4314(10), 3.3839(6) or 3.3184(5) Å appears in **2a**, **4** or **6**, respectively, between adjacent antiparallel molecules resulting in couples (see figures 6-8). These Au-Au distances are in general longer than in other gold(I) complexes which display intermolecular unsupported interactions.[8] These couples are packed in the solid state forming chains (that in the case of **2a** run parallel to the crystallographic *x* axis) in which the orientation of adjacent molecules is in an antiparallel fashion (or parallel couples) and in which there are no further Au-Au contacts.

The second polymorph of complex **2** (**2b**), contains discrete molecules in which the aromatic rings, instead of being coplanar, form an angle of 45.07° (Figure 9). As in the **2a**, the molecules are packed forming chains that run parallel to the crystallographic *x* axis but without metal-metal

interactions (the shortest Au-Au distance being 3.8104(2) Å) and with the same orientation of the dipoles.

Finally, the asymmetric unit of complex **3** contains four molecules in which the perhalophenyl and tertbutylpyridine rings form angles between 16.73 and 47.82° (see Figure 10) and that are associated in couples of nearly parallel molecules via unsupported Au...Au interactions of 3.1062(5) and 3.1155(5) Å, that is, shorter than in **2a**, **4** or **6** (see table 3). These pairs of molecules are packed in the net in an antiparallel fashion forming chains in which the shortest gold-gold distance of 3.9128(8) Å is too long to consider the presence of any other metallophillic interaction.

## DFT calculations

In the introduction we have mentioned all the factors that can affect the luminescence in gold complexes. The result of the experimentally observed emissions for the isolated complexes **1-6** is surprisingly simple, since one would expect a more complicated sequence of groups and energies. The DFT calculations are employed to explain how the different factors affect in the emission energy by the analysis of the HOMO-LUMO gap on the corresponding electronic structures.

We have employed three types of model systems in order to rationalize the factors that could affect or not the luminescence of these gold(I) complexes. First, we have analysed the mononuclear model systems [Au($C_6Cl_5$)(4-Me-py)] and [Au($C_6Cl_5$)(4-CN-py)] in which we compare the effect of the substituent in the position 4 of the pyridine ring on the HOMO-LUMO gap and on the character of these frontier orbitals. Then we have compared the effect of having gold-gold interactions on the compounds building up model systems $[Au(C_6Cl_5)(4\text{-Me-py})]_2$ and $[Au(C_6Cl_5)(4\text{-CN-py})]_2$ through the obtained X-ray structural parameters and comparing them with mononuclear models [Au($C_6Cl_5$)(4-Me-py)] and [Au($C_6Cl_5$)(4-CN-py)], respectively. Finally, we have also built up the polymorphic parallel and antiparallel model systems corresponding to the dimer $[Au(C_6Cl_5)(4\text{-Me-py})]_2$ in order to check whether the dipole disposition of the mononuclear counterparts affects or not the HOMO-LUMO gap.

First, the effect of the substituent on the pyridine is analyzed. To do that we compare the electronic structure of the mononuclear cyanopyridine complex with the methylpyridine complex. The orbitals of lower energies are in both cases located in the perhalophenyl groups and in the gold center (HOMO-2). By contrast, the LUMO orbitals are located in the pyridine rings. The main difference is the position of the LUMO orbital that, in the case of the methyl derivative, is placed higher in energy making the HOMO-LUMO transition more energetic as we observed experimentally. Therefore, the obtained sequence would be logical if all the structures were isolated molecules since the only analyzed factor responsible for the LUMO energies is the substituent on the pyridine ring.

But there are different structures and most of them display gold-gold interactions. We have compared the mononuclear model with the cyano substituent and the structure obtained by X-ray diffraction studies which shows a gold-gold

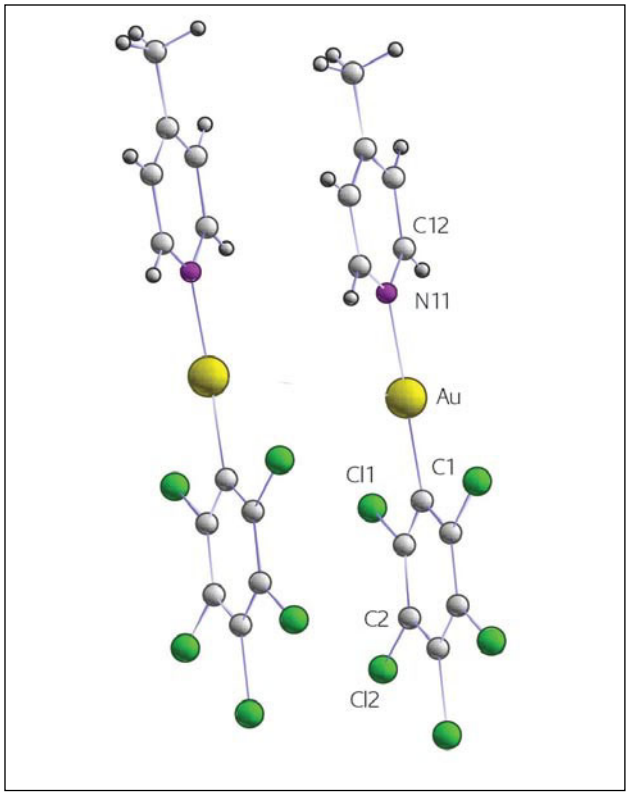


**Figure 9**
*Crystal structure of complex **2b***

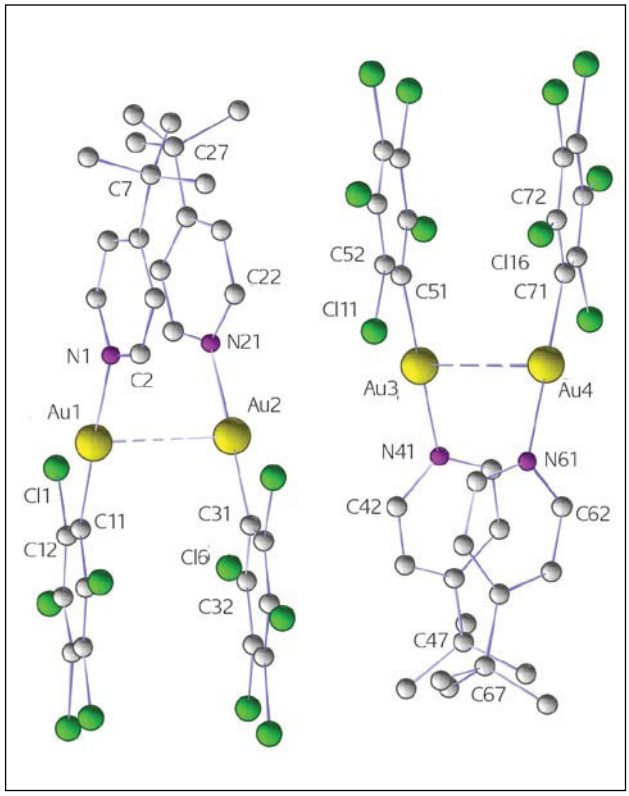


**Figure 10**
*Crystal structure of complex **3***

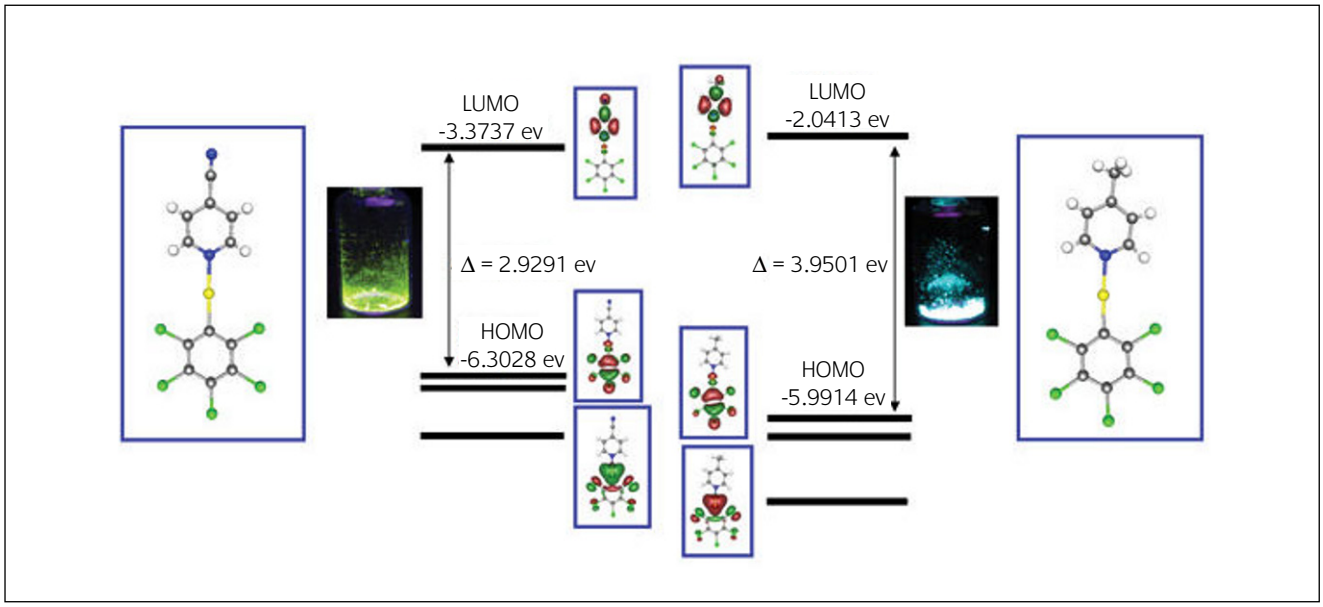


**Figure 11**

*Frontier orbitals schemes for model systems [Au($C_6Cl_5$)(4-Me-Py)] and [Au($C_6Cl_5$)(4-CN-Py)*

interaction of 3.3 Å. The overlapping of the orbitals produces an increase both in the HOMO as in the LUMO energies, but with a different composition. Thus, in the case of the LUMO, again it is located in the pyridine rings, but the HOMO is mainly formed by orbitals of the gold centres that increase their energies compared to the one found in the monomer. The relative increment of both makes the HOMO and LUMO gap almost equal and, therefore, the presence of gold-gold interactions does not affect the energies of the emissions, although it does their compositions.

To be sure that this effect is not a particular case of the cyano derivative this calculation was repeated with the methyl substituent, finding a similar behavior, both in equal energies for the monomer and the dimer, and in the composition of the frontier orbitals.

Finally, a third factor that can be studied is the existence of two polymorphs in pentachlorophenyl-4-methylpyridinegold(I) depending on the crystallization process. Thus, when the crystallization is rapid, for example, by precipitation, the isomer obtained has an antiparallel disposition of the dipoles, but a longer crystallization process gives rise to a mixture of crystals from which the other polimorph can be separated. Curiously, both isomers show different emissions, the antiparallel molecule being almost 30 nm more energetic.

Indeed, the molecular orbital diagram of the antiparallel form displays a gap of 4 electron-volts while the parallel one of 3.24, which is in accordance with the more energetic emission of the former observed experimentally. In this case the composition of the orbitals is also different and, while in the antiparallel form the HOMO is composed mainly of $d_{z^2}$ orbitals of gold, in the case of the parallel, this orbital is mostly located in the pentachlorophenyl rings.

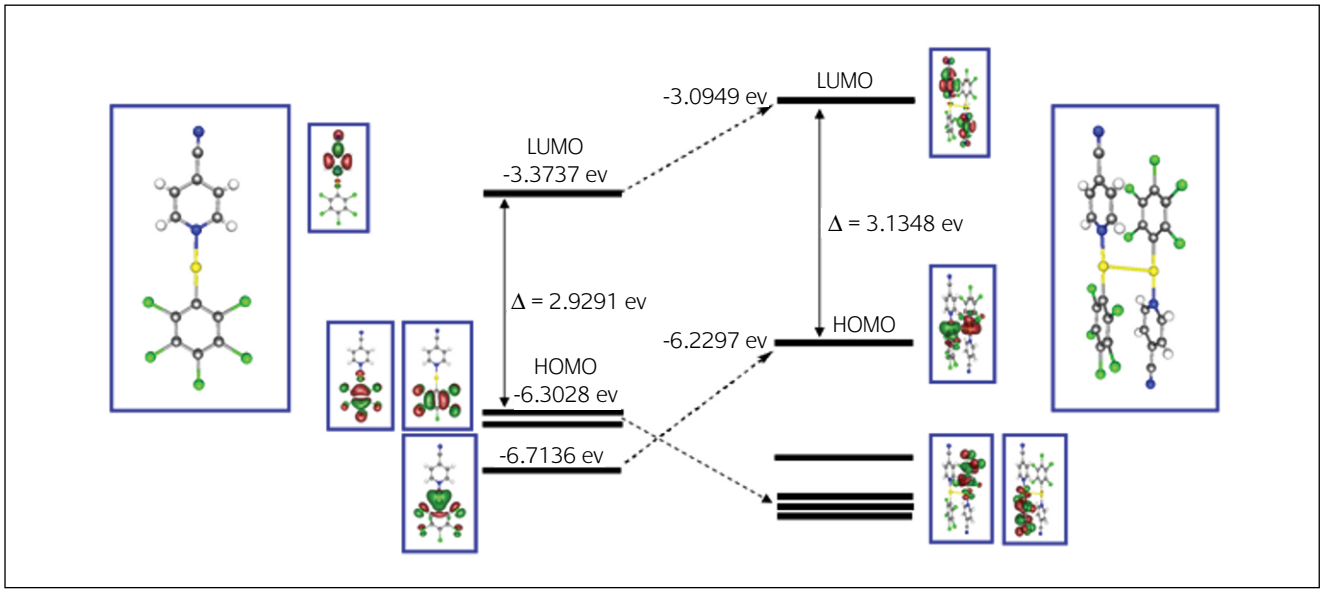


**Figure 12**

*Frontier orbitals schemes for model systems [Au($C_6Cl_5$)(4-CN-Py)] and [Au($C_6Cl_5$)(4-CN-Py)]$_2$)*

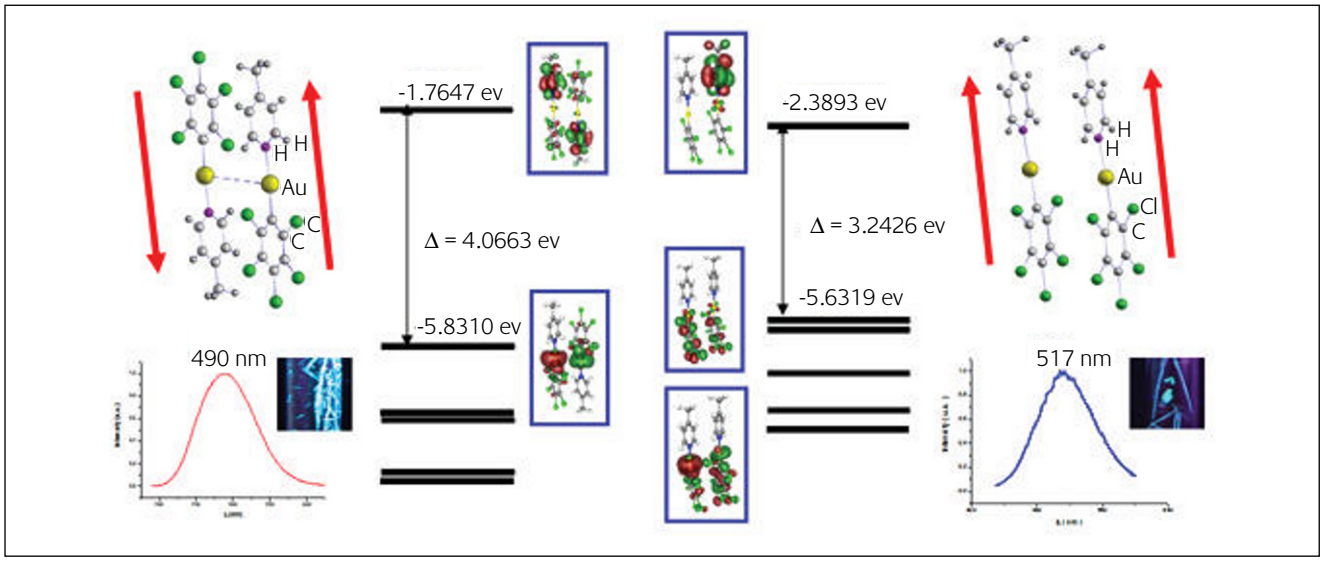


**Figure 13**

*Frontier orbitals schemes for model systems $[Au(C_6Cl_5)(4\text{-Me-Py})]_2$ (antiparallel disposition) and $[Au(C_6Cl_5)(4\text{-Me-Py})]_2$ (parallel disposition)*

After the structural and the theoretical analysis of the different factors that can affect the luminescence on these complexes one is tempted to rationalize the reasons why the dipoles align the way they do as a function of the substituents in the pyridine rings. Nevertheless, there is no evident correlation about that since most of the structures adopt the antiparallel disposition of the dipoles, the 4-methyl-pyridine compound presents two polymorphs with parallel and antiparallel disposition of the dipoles and, finally, the exception is achieved in the tert-butyl substituted derivative in which an almost parallel disposition of the dipoles is obtained between molecules together with an antiparallel disposition between couples of molecules as shown in Figure 10. This trend would be rationalized in terms of a delicate balance between weak aurophillic and π–π stacking interactions (between similar or different rings) and packing effects in which both the electronic and steric effects of the subsituents in position 4 of the pyridine rings would be important. Related with the aromatic stacking it should be pointed out that the dipole assisted formation of π–π stacking between different types of aromatic rings as $C_6Cl_5$ and pyridine would favour the antiparallel disposition in this type of complexes. In this sense, several studies on free $C_6F_6$-benzene stacking interactions have been carried out and, among them, a recent study reported by BW Gung et al[9] on the substituent effects in $C_6F_6...C_6H_5X$ stacking interactions shows that electron donating groups increase and electron-withdrawing groups decrease the interaction energies. In our case, it is difficult to assess this possibility since, as we have mentioned before, there are other factors as coordination to

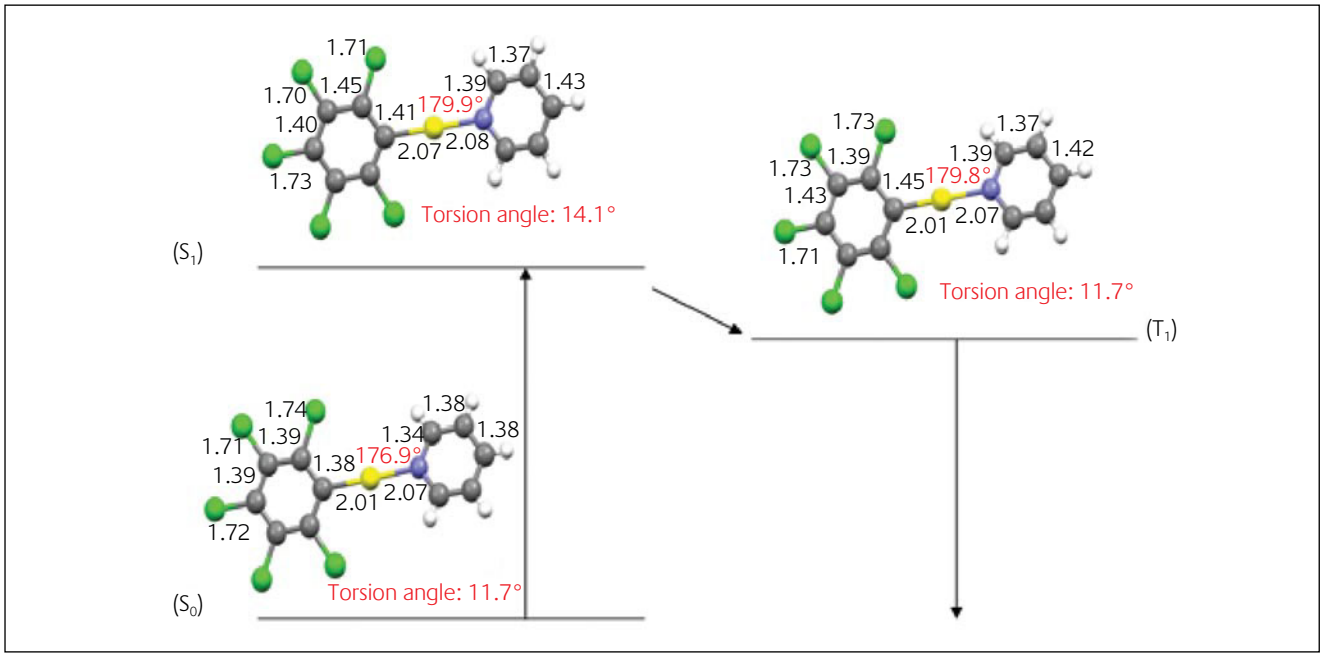


**Figure 14**

*TD-DFT optimized structures for model $[Au(C_6Cl_5)(Py)]$ in the lowest singlet and lowest triplet excited states*

gold(I), aurophilicity, packing forces, etc that would permit to isolate the polymorphs in different dispositions. Nevertheless, the presence of such interactions would play a significant role on the structural dispositions.

## Excited state structure

All the complexes show mono-exponential decays with lifetimes in the microseconds range (table 1). These are in accordance with phosphorescent processes from excited states of triplet parentage. Therefore, taking all the presented data into account, we assign the emissions to arise from a Ligand-Metal($C_6Cl_5$-Au)-to-Ligand(Pyridine)-Charge-Transfer Transitions (LMLCT).

The time dependent DFT calculations on a model system taken from the X-ray data for complex **4** allow to optimize the structure of the molecule in the excited states. Thus, the transition between the ground and the first single state produces a slight enlargement of the Au-C distance from 2.01 to 2.07 and an evident rupture of the aromaticity in both rings, which is in accordance with an electronic transition involving π-density between both groups. Also, the torsion angle between ground and the first single state increases from 11.7° to 14.1°.

A non-radiative intersystem crossing takes the molecule to the triplet state, where the rupture of the aromaticity remains and the torsion angle reaches similar values than in the ground state. Taking the experimental data into account, it seems likely that the emission is produced from this state.

## Conclusions

To summarize, these results are indicative of a very promising area of research, because the synthesis of these organometallic Au(I) compounds is very simple and the products show a great stability and potential for practical applications. Indeed, the simplicity of the synthesized compounds permits to carry out a deep analysis of the photophysical properties of the new complexes both from an experimental and a theoretical viewpoint. Thus, the change on the substituents in 4 position of the pyridine ligands bonded to gold permits to modulate the luminescence of the different species giving rise to a clear correlation between their donor properties and the emission energies. The emissions rise following the trend MeO > Me > tBu > H > COOMe > CN. Another interesting feature is that it is also possible to tune the photophysical properties through the synthesis of products in which the relative orientation of the molecules leads to different emissions.

## Experimental

**General.** The compound [Au($C_6Cl_5$)(tht)] was prepared by reported literature methods.[10] The starting materials were purchased from Sigma-Aldrich and Acros Organics and used as received.

**Instrumentation.** Infrared spectra were recorded in the range 4000-200 $cm^{-1}$ on a Perkin-Elmer FT-IR Spectrum 1000 spectrophotometer using Nujol mulls between polyethylene sheets. C, H, N, S analyses were carried out with a C.E. Instrument EA-1110 CHNS-O microanalyser. $^1$H NMR spectra were on a Bruker ARX 300 in $CDCl_3$. Chemical shifts are quoted relative to $SiMe_4$ ($^1$H external). Absorption spectra in solution were registered on a Hewlett Packard 8453 Diode Array UV-visible spectrophotometer. Excitation an emission spectra as well as lifetime measurements were recorded with a Jobin-Yvon Horiba Fluorolog 3-22 Tau-3 spectrofluorimeter.

**Preparation of the Complexes [Au($C_6Cl_5$)L] (L = 4-MeO-Py, 1; 4-Me-Py, 2; 4-$^t$Bu-Py, 3; Py, 4; 4-COOMe-Py, 5; 4-CN-Py,6).** To a dichloromethane solution (20 ml) of [Au($C_6Cl_5$)(tht)] (0.09 g, 0.168 mmol) was added 4-MeO-Py (18.3 mg, 0.168 mmol), **1**; 4-Me-Py (15.6 mg, 0.168 mmol), **2a**; 4-$^t$Bu-Py (22.7 mg, 0.168 mmol), **3**; Py (13.3 mg, 0.168 mmol), **4**; 4-COOMe-Py (23 mg, 0.168 mmol), **5**; 4-CN-Py (17 mg, 0.168 mmol), **6**. After 30 minutes of stirring at room temperature the solvent was evaporated to *ca*. 5ml. Addition of *n*-hexane (15 mL) led to precipitation of the resulting solids that were isolated by filtration (yields ~ 75%, **1**; 65%, **2a**; 48%, **3**; 44%, **4**; 58%, **5**; 43%, **6**). In the case of complex **2a** a new polymorph **2b** can be obtained through a slow crystallization process.

Complexes **1-5** are obtained as white solids, whereas **6** is yellow.

Experimental data for **1**: Elemental analysis (%) calcd. for $C_{12}H_7AuCl_5NO$: C, 25.95; H, 1.27; N, 2.52. Found: C, 25.65; H, 1.37; N, 2.46. $^1$H NMR (298K, $CDCl_3$) δ 3.95 (s, 3H, CH3), δ 7.00 (d, 2H, $H_m$), δ 8.45 (d, 2H, $H_o$). FT-IR (Nujol mulls): ν 1612 $cm^{-1}$ (C=N), ν 838, 630 $cm^{-1}$ (Au-$C_6Cl_5$).

Experimental data for **2a**: Elemental analysis (%) calcd. for $C_{12}H_7AuCl_5N$: C, 26.72; H, 1.31; N, 2.06. Found: C, 26.69; H, 1.38; N, 1.92. $^1$H NMR (298K, $CDCl_3$) δ 2.47 (s, 3H, $CH_3$), δ 7.36 (d, 2H, $H_m$), δ 8.47 (d, 2H, $H_o$). FT-IR (Nujol mulls): ν 1622 $cm^{-1}$ (C=N), ν 845, 628 $cm^{-1}$ (Au-$C_6Cl_5$).

Experimental data for **3**: Elemental analysis (%) calcd. for $C_{15}H_{13}AuCl_5N$: C, 30.98; H, 2.25; N, 2.41. Found: C, 30.96; H, 2.13; N, 2.21. $^1$H NMR (298K, $CDCl_3$) δ 1.35 (s, 9H, $CH_3$), δ 7.53 (d, 2H, $H_m$), δ 8.52 (d, 2H, $H_o$). FT-IR (Nujol mulls): ν 1616 $cm^{-1}$ (C=N), ν 830, 628 $cm^{-1}$ (Au-$C_6Cl_5$).

Experimental data for **4**: Elemental analysis (%) calcd. for $C_{11}H_5AuCl_5N$: C, 25.15; H, 0.96; N, 2.67. Found: C, 24.84; H, 0.92; N, 2.51. $^1$H NMR (298K, $CDCl_3$) δ 8.00 (m, 1H, $CH_3$), δ 7.6 (m, 2H, $H_m$), δ 8.66 (d, 2H, $H_o$). FT-IR (Nujol mulls): ν 1604 $cm^{-1}$ (C=N), ν 846, 632 $cm^{-1}$ (Au-$C_6Cl_5$).

Experimental data for **5**: Elemental analysis (%) calcd. for $C_{13}H_7AuCl_5NO_2$: C, 26.76; H, 1.21; N, 2.40. Found: C, 26.56; H, 1.12; N, 2.28. $^1$H NMR (298K, $CDCl_3$) δ 4.03 (s, 3H, $CH_3$), δ 8.14 (d, 2H, $H_m$), δ 8.83 (d, 2H, $H_o$). FT-IR (Nujol mulls): ν 1616 $cm^{-1}$ (C=N), ν 846, 630 $cm^{-1}$ (Au-$C_6Cl_5$), ν 1737 $cm^{-1}$ (C=O).

Experimental data for **6**: Elemental analysis (%) calcd. for $C_{12}H_4AuCl_5N$: C, 26.87; H, 0.75; N, 2.61. Found: C, 26.82; H,

**Table 2**
*Data collection and structure refinement details for complexes **2**, **3**, **4** and **6***

| Compound | 2(a) | 2(b) | 3 | 4 | 6 |
|---|---|---|---|---|---|
| Chemical Formula | $C_{12}H_7AuCl_5N$ | $C_{12}H_7AuCl_5N$ | $C_{15}H_{13}AuCl_5N$ | $C_{11}H_5AuCl_5N$ | $C_{12}H_4AuCl_5N_2$ |
| Crystal habit | Colorless cube | Colorless prism | Colorless plate | Colorless prism | Yellow cube |
| Crystal size/mm | 0.18 x 0.15 x 0.15 | 0.4 x 0.3 x 0.3 | 0.2 x 0.18 x 0.04 | 0.23 x 0.18 x 0.13 | 0.06 x 0.06 x 0.06 |
| Crystal system | Triclinic | Triclinic | Triclinic | Monoclinic | Monoclinic |
| Space group | P-1 | P-1 | P-1 | $P2_1/c$ | $P2_1/c$ |
| *a*/Å | 7.122(2) | 3.810(1) | 13.084(2) | 7.657(3) | 15.274(3) |
| *b*/Å | 7.771(2) | 13.159(3) | 16.627(3) | 23.509(8) | 13.990(4) |
| *c*/Å | 14.885(4) | 14.242(3) | 19.423(4) | 8.084(3) | 14.375(4) |
| α/° | 77.080(11) | 86.185(9) | 112.644(10) | 90 | 90 |
| β/° | 77.260(10) | 83.825(9) | 98.897(10) | 111.84(1) | 104.733(14) |
| γ/° | 69.867(16) | 88.438(14) | 105.603(10) | 90 | 90 |
| *U*/Å$^3$ | 744.52(3) | 708.26(3) | 3594.04(11) | 1350.72(9) | 2972.03(13) |
| *Z* | 2 | 2 | 8 | 4 | 8 |
| $D^c$/g cm$^{-3}$ | 2.406 | 2.529 | 2.149 | 2.584 | 2.460 |
| *M* | 539.40 | 539.40 | 581.48 | 525.38 | 550.39 |
| *F*(000) | 500 | 500 | 2192 | 968 | 2032 |
| *T*/°C | -100 | -100 | -100 | -100 | -100 |
| $2\theta_{max}$/° | 56 | 56 | 56 | 56 | 56 |
| μ(Mo-*K*α)/mm$^{-1}$ | 10.759 | 11.310 | 8.924 | 11.857 | 10.786 |
| No. of reflections measured | 11043 | 11809 | 50257 | 6539 | 26782 |
| No. of unique reflections | 1411 | 3327 | 17058 | 3034 | 7245 |
| $R_{int}$ | 0.0392 | 0.0491 | 0.0829 | 0.0620 | 0.0602 |
| $R^a$ (I>2σ(I)) | 0.0236 | 0.0270 | 0.0559 | 0.0305 | 0.0505 |
| $wR^b$($F^2$, all refl.) | 0.0565 | 0.0678 | 0.1382 | 0.0727 | 0.0981 |
| No. of parameters | 189 | 186 | 805 | 163 | 361 |
| No. of restraints | 74 | 56 | 240 | 52 | 118 |
| $S^c$ | 1.055 | 1.076 | 1.019 | 1.067 | 1.038 |
| Max. Δρ/eÅ$^{-3}$ | 1.286 | 1.559 | 1.888 | 0.986 | 3.888 |

[a] $R(F) = \Sigma \,||F_O| - |F_C|| / \Sigma\, |F_O|$. [b] $wR(F^2) = [\Sigma\{w(F_O^2-F_C^2)^2\}/\Sigma\{w(F_O^2)^2\}]0.5$; $w^{-1} = \sigma^2(F_O^2)+(aP)^2+bP$, where $P = [F_O^2+2F_C^2]/3$ and α and *b* are constants adjusted by the program. [c] $S = [\Sigma\{w(F_O^2-F_C^2)^2\}/(n-p)]^{0.5}$, where *n* is the number of data and *p* the number of parameters

0.70; N, 2.52. $^1$H NMR (298K, $CDCl_3$) δ 7.86 (d, 2H, $H_m$), δ 8.90 (d, 2H, $H_o$).

**Computational Details for DFT and TD-DFT calculations.** The model systems used in the theoretical studies were taken from the X-ray diffraction data for complexes **2a, 2b** and **6** respectively or by full optimization at DFT level of model systems corresponding to free pyridines 4-X-Py (X = MeO-, Me-, H-, CN-) or the model system that represents the gold precursor [Au($C_6Cl_5$)($SH_2$)]. Keeping all distances, angles and dihedral angles frozen, single-point DFT calculations were performed on all model systems. In both the ground-state calculations and the subsequent optimization of the lowest triplet excited state for complex **4**, the B3LYP functional[11] as implemented in TURBOMOLE[12] was used. The excitation energies were obtained at the density functional level by using the time-dependent perturbation theory approach (TD-DFT).[13] In all calculations, the Karlsruhe split-valence quality basis sets[14] augmented with polarization functions[15] were used (SVP). The Stuttgart effective core potential in TURBOMOLE was used for Au.[16]

**Crystallography.** The crystals were mounted in inert oil on glass fibbers and transferred to the cold gas stream of a Nonius Kappa CCD diffractometer equipped with an Oxford Instruments low-temperature attachment. Data were collected by monochromated Mo Kα radiation (λ = 0.71073 Å). Scan type ω and ϕ. Absorption corrections: numerical (based on multiple scans). The structures were solved by direct methods and refined on $F^2$ using the program SHELXL-97.[17] All non-hydrogen atoms were anisotropically refined and hydrogen atoms were included using a mixed model. Further

**Table 3**
*Selected bond lengths [Å] and angles [º]*

| Complex | Au-C | Au-N | C-Au-N | Au···Au |
|---|---|---|---|---|
| **2a** | 2.003(6) | 2.068(5) | 175.8(2) | 3.4314(10) |
| **2b** | 2.003(4) | 2.063(4) | 176.0(2) | --- |
| **3** | 2.017(7) | 2.085(7) | 177.2(3) | 3.1062(5) |
| | 2.004(8) | 2.062(7) | 179.7(3) | |
| | 1.989(8) | 2.070(6) | 179.3(3) | 3.1155(5) |
| | 2.006(8) | 2.062(7) | 177.1(3) | |
| **4** | 2.014(5) | 2.070(4) | 176.9(2) | 3.3839(6) |
| **6** | 2.031(8) | 2.074(6) | 178.7(3) | 3.3184(5) |
| | 2.013(8) | 2.072(6) | 176.6(3) | |

details on the data collection and refinement methods can be found in Table 2. Selected bond lengths and angles are shown in Table 3. CCDC-632363-632367 contain the supplementary crystallographic data for this paper. These data can be obtained free of charge via www.ccdc.cam.ac.uk/conts/retrieving.html (or from the Cambridge Crystallographic Data Centre, 12 Union Road, Cambridge CB2 1EZ, UK; fax: (+44) 1223-336-033; or e-mail: deposit@ccdc.cam.ac.uk).

## Acknowledgement

The D.G.I. MEC/FEDER (CTQ2004-05495) is thanked for financial support. M. Monge thanks the MEC-Universidad de La Rioja for his research contract "Ramón y Cajal". M. Montiel and M. Rodríguez-Castillo thank the C.A.R. for a grant.

## About the authors

The group in the University of La Rioja is working in gold chemistry since 1979 and they have produced more than 80 scientific papers and two patents. They focus their interest not only in the synthesis of new homo- and hetero-nuclear gold compounds, but also in the study of some properties such as luminescence or biomedical behaviour and in the application of theoretical calculations. Some of them have been invited to give talks at different International Conferences or Universities in America, Asia or Europe.


**EJ Fernández**


**A Laguna**


**JM López de Luzuriaga**


**M Monge**


**M Montiel**

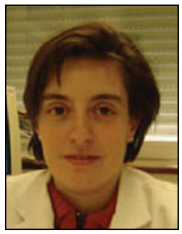
**ME Olmos**


**J Pérez**


**M Rodriguez-Castillo**

## References

1 a) Ward, M. D.; White, C. M.; Barigelletti, F.; Armaroli, N.; Calogero, G.; Flamigni, L. *Coord. Chem. Rev.* **1998**, *171*, 481-488. b) Balzani, V.; Juris, A.; Venturi, M.; Campagna, S.; Serroni, S. *Chem. Rev.* **1996**, *96*, 759-833

2 a) Farha, F.; Iwamoto, R. T. *Inorg. Chem.* **1965**, *4*, 844. b) Catalano, V. J.; Horner, S. J. *Inorg. Chem.* **2003**, *42*, 8430. c) Catalano, V. J.; Moore, A. L. *Inorg. Chem.* **2005**, *44*, 6558

3 Schmidbaur, H. in Gold - *Progress in Chemistry, Biochemistry and Technology*, John Wiley & Sons, Inc., New York, 1999

4 Schmidbaur, H.; Graf, W.; Müller, G. *Angew. Chem., Int. Ed. Engl.* **1988**, *27*, 417

5 Forward, J. M.; Fackler, J. P., Jr.; Assefa, Z. in *Optoelectronic Properties of Inorganic Compounds* (Eds.: Roundhill, D.M.; Fackler, J.P., Jr.), Plenum, New York, 1999, pp 195-226

6 See for example: a) Fernández, E. J.; Laguna, A.; López-de-Luzuriaga, J. M.; Monge, M.; Montiel, M.; Olmos, M. E. *Inorg. Chem.* **2005**, *44*, 1163. b) Fernández, E. J.; Laguna, A.; López-de-Luzuriaga, J. M.; Monge, M.; Montiel, M.; Olmos, M. E.; Rodríguez-Castillo, M. *Organometallics* **2006**, *25*, 3639. c) Fernández, E. J.; Laguna, A.; López-de-Luzuriaga, J. M.; Monge, M.; Montiel, M.; Olmos, M. E.; Pérez, J.; Puelles, R. C.; Sáenz, J. C. *Dalton Trans.* **2005**, 1162. d) Fernández, E. J.; López-de-Luzuriaga, J. M.; Monge, M.; Olmos, M. E.; Pérez, J.; Laguna, A. *J. Am. Chem. Soc.* **2002**, *124*, 5942. e) Fernández, E. J.; López-de-Luzuriaga, J. M.; Monge, M.; Olmos, M. E.; Pérez, J.; Laguna, A.; Mohamed, A. A.; Fackler, J. P., Jr. *J. Am. Chem. Soc.* **2003**, *125*, 2022. f) Fernández, E. J.; Laguna, A.; López-de-Luzuriaga, J. M.; Olmos, M. E.; Pérez, *J. J. Chem. Commun.* **2003**, 1760

7 Fernández, E.J.; Laguna, A.; López-de-Luzuriaga, J. M. *Coord. Chem. Rev.* **2005**, *249*, 1423 and references therein

8 Fernández, E. J.; Laguna, A.; Olmos, M. E. *Adv. Organomet. Chem.*, **2005**, *52*, 77

9 Gung, B. W.; Amicangelo, J. C. *J. Org. Chem.* **2006**, *71*, 9261

10 Usón, R.; Laguna, A.; Vicente, J.; García, J.; Bergareche, B. *J. Organomet. Chem.* **1979**, *173*, 349

11 a) Becke, A. D. *J. Chem. Phys.*, **1992**, *96*, 215. b) Becke, A. D. *J. Chem. Phys.*, **1993**, *98*, 5648. c) Lee, C.; Yang, W.; Parr, R. G. *Phys. Rev. Lett.*, **1998**, *B 37*, 785

12 Ahlrichs, R.; Bär, M.; Häser, M.; Horn, H.; Kölmel, C. *Chem. Phys. Lett.*, **1989**, *162*, 165

13 a) Bauernschmitt, R.; Ahlrichs, R. *Chem. Phys. Lett.*, **1996**, *256*, 454 b) Bauernschmitt, R.; Ahlrichs, R. *J. Chem. Phys.*, **1996**, *104*, 9047 c) Bauernschmitt, R.; Häser, M.; Treutler, O.; Ahlrichs, R. *Chem. Phys. Lett.*, **1997**, *264*, 573 and refs. therein. d) Gross, E. K. U.; Kohn, W. *Advan. Quantum Chem.* **1990**, *21*, 255. e) Casida, M. E. in *Recent advances in density functional methods*, Vol 1, (Ed.: D. P. Chong), World Scientific, 1995

14 Schäfer, A.; Horn, H.; Ahlrichs, R. *J. Chem. Phys.* **1992**, *97*, 2571

15 Dunning, T. H., Jr., *J. Chem. Phys.* **1994**, *100*, 5829

16 Andrae, D.; Haeussermann, U.; Dolg, M.; Stoll, H.; Preuss, H. *Theor. Chim. Acta* **1990**, *77*, 123

17 Sheldrick, G. M.; University of Göttingen: Göttingen, Germany, **1997**